EFFICIENT ION HEATING OF TOKAMAK PLASMA BY APPLICATION OF POSITIVE AND NEGATIVE CURRENT PULSE IN TRIAM-1

Toi, Kazuo
Research Institute for Applied Mechanics, Kyushu University : Associate Professor

Hiraki, Naoji
Research Institute for Applied Mechanics, Kyushu University : Research Associate

Nakamura, Kazuo
Research Institute for Applied Mechanics, Kyushu University : Research Associate

Mitarai, Osamu
Research Institute for Applied Mechanics, Kyushu University

他

https://doi.org/10.5109/6617936

出版情報：Reports of Research Institute for Applied Mechanics. 27 (86), pp.111-123, 1979-12. 九州大学応用力学研究所

Reports of Research Institute for Applied Mechanics
Vol. XXVII, No. 86, 1980

EFFICIENT ION HEATING OF TOKAMAK PLASMA BY APPLICATION OF POSITIVE AND NEGATIVE CURRENT PULSE IN TRIAM-1

by Kazuo TOI*, Naoji HIRAKI**, Kazuo NAKAMURA**, Osamu MITARAI***, Yoshinobu KAWAI*, and Satoshi ITOH****

The efficient heating of bulk ions of tokamak plasma is observed by application of the pulsed toroidal electric field much higher than the Dreicer field with the positive and negative polarities for the ohmic heating field. No deleterious effect on the confinement properties of tokamak plasma appears by the heating. The decay time of ion temperature raised by the heating pulse agrees well with the prediction by the neoclassical transport theory. The magnitude of the current induced by the pulsed electric field with the positive polarity is limited by the violent current disruption. In the case of the negative polarity, this is limited by lack of the MHD equilibrium due to vanishing the total plasma current. The ratio of drift velocity to electron thermal one $\langle u_d \rangle / \langle v_{the} \rangle$ attains around 0.5, which suggests that the efficient ion heating may be due to the current-driven turbulence.

Key words: tokamak plasma, ion heating, pulsed toroidal electric field, Dreicer field, neoclassical transport theory, current-driven turbulence

1. Introduction

Many additional heating methods are proposed and investigated theoretically and experimentally to heat an ohmically heated tokamak plasma up to the ignition state. Especially, neutral beam injection[1)~3)] and wave heating in the lower hybrid frequency range[4)] and ion cyclotron frequency range[5)] have been applied to many tokamaks. These experiments show that the above additional heating methods are effective for

* Associate Professor, Research Institute for Applied Mechanics, Kyushu University.
** Research Associate, Research Institute for Applied Mechanics, Kyushu University.
*** JSPS Post Doctoral Fellowships (General), Research Institute for Applied Mechanics, Kyushu University.
**** Professor, Research Institute for Applied Mechanics, Kyushu University.

heating tokamak plasmas. The turbulent heating by a pulsed high current along the toroidal magnetic field may also be promissing to heat the tokamak plasma. This heating method is advantageous for minimizing and simplifying the additional heating system of tokamak plasma. Since early stage of fusion research, the turbulent heating has been carried out by application of the high electric field ($E_t \gtrsim 100$ V/cm) in the various types of toroidal plasma on rather short time-scale less than several micro-seconds[6)~9)] and has been successful in producing the interesting plasma densities and/or temperatures to a certain extent. In all cases, however, the turbulent heating has been applied to plasmas in the low temperature range ($\lesssim 20$ eV) and the heated plasma has not been stably maintained for more than several times of the heating-pulse duration due to the remarkable energy losses. It is required from the reactor aspect that the turbulent heating by the lower electric field is carried out for high temperature plasma of the longer time-scale without deterioration of confinement properties.

This paper describes the experimental results when the relatively low magnitude of the electric field pulse ($\lesssim 10$ V/cm) is applied to the stably confined tokamak plasma produced by ohmic heating in TRIAM-1.

2. Experimental Device and Diagnostic Methods

The TRIAM-1[10)11)] is a small high-field tokamak with the ratio of toroidal magnetic field to major radius of plasma $B_t/R \simeq 16$ T/m (Tab. 1).

Table 1. Characteristic parameters of TRIAM-1

Major plasma radius	: $R=25.4$ cm
Minor radius of vacuum chamber	: $b=5.3$ cm
Minor plasma radius (defined by molybdenum limiter)	: $a=4$ cm
Toroidal magnetic field	: $B_t=40$ kG
Skin time of shell (vacuum chamber)	: $\tau_s=160$ μsec
Pulsed electric field for turbulent heating	: $E_t \lesssim 10$ V/cm
Rise time of the pulsed current	: $\tau_r=4$ μsec
Equivalent duration time of the pulsed current	: $T=8$ μsec
Two ceramic breaks are equipped on the vacuum chamber.	

The ratio is larger than that of Alcator device[12)]. Therefore, it is advantageous for achieving the high plasma current density. The radius (a) is defined by a molybdenum limiter of which aperture radius is 4 cm. The equilibrium position of the plasma is essentially maintained by the pre-programmed vertical and horizontal fields, since the vacuum chamber only acts as the resitive shell with a skin time of 160 μsec. The primary coil for the turbulent heating consists of four parallel poloidal loops which are located just outside the vacuum chamber and in the bore of toroidal coils. The position and current-allocation of each loop are determined to maximize a coupling coefficient between the coil and a plasma. The vacuum chamber is insulated to the toroidal direction by two ceramic breaks. The e-fold rise time of the pulsed plasma current is about 4 μsec and the equivalent rectangular pulse length is about 8 μsec. The perpendicular ion temperature ($T_{i\perp}$) is obtained by a neutral atom energy analyzer (NEA) which can be scanned from $z=+4$ cm (top) to -4 cm (bottom)[13]. The electron temperature on the plasma axis (T_{eo}) is measured by Thomson scattering. The line-average electron density ($\bar{n}_e$) is monitored by 2 mm-microwave interferometer[14]. The one-turn loop and Rogowskii coil with response up to 10 MHz including the electronic circuits[15] are used for measurement of the pulsed loop voltage (V_{loop}^{TH}) and plasma current (I_p^{TH}) induced by the heating pulse.

3. Experimental Results

The tokamak plasma with the following parameters is produced by ohmic heating (solid curves in Fig. 1(a)), i.e., ohmic heating current $I_p \simeq$ 21 kA, toroidal magnetic field $B_t \simeq 26$ kG, safety factor at plasma surface $q(a) \simeq 4$, line-average electron density $\bar{n}_e \simeq 2.1 \times 10^{13}$ cm^{-3}, and central electron and ion temperatures $T_{e0} \simeq 250$ eV and $T_{i0} \simeq 140$ eV, respectively. In this discharge the MHD activity monitored by magnetic probes is in a sufficiently low level ($[\widetilde{\delta B_\theta}/B_\theta]_a < 0.1\%$). In this high temperature plasma, the pulsed electric field with the positive polarity has been superimposed on the ohmic heating field at 2.5 msec (broken curves in Fig. 1(a) and Fig. 1(b)). Though the applied electric field is relatively low ($E_t \simeq 7$ V/cm), it is much higher than the Dreicer field E_D because of high electron temperature and relatively low electron density. Figure 1(b) shows the plasma current (I_p^{TH}) and loop voltage (V_{loop}^{TH}), induced by the heating pulse. In this paper, we pay attention to only time behaviour of plasma parameters, cxcept for applied interval of the heating pulse.

As is seen from Fig. 1(a), though the waveform of ohmic heating current (I_p) does not change after application of the heating pulse, the loop voltage (V_{loop}) decreases by about 20% after 0.5 msec and average electron density ($\bar{n}_e$) increases by about 15% after 0.7 msec. It is considered that the increase in density is responsible for impurity influx which results from the skin heating.

Figure 2 shows the energy spectra of fast neutral atoms emitted from the central position ($z=0$) for both cases without and with the heating pulse during 0.1 to 0.2 msec after the pulse. Both energy spectra indicate two groups with different "temperature". The bulk ion tem-

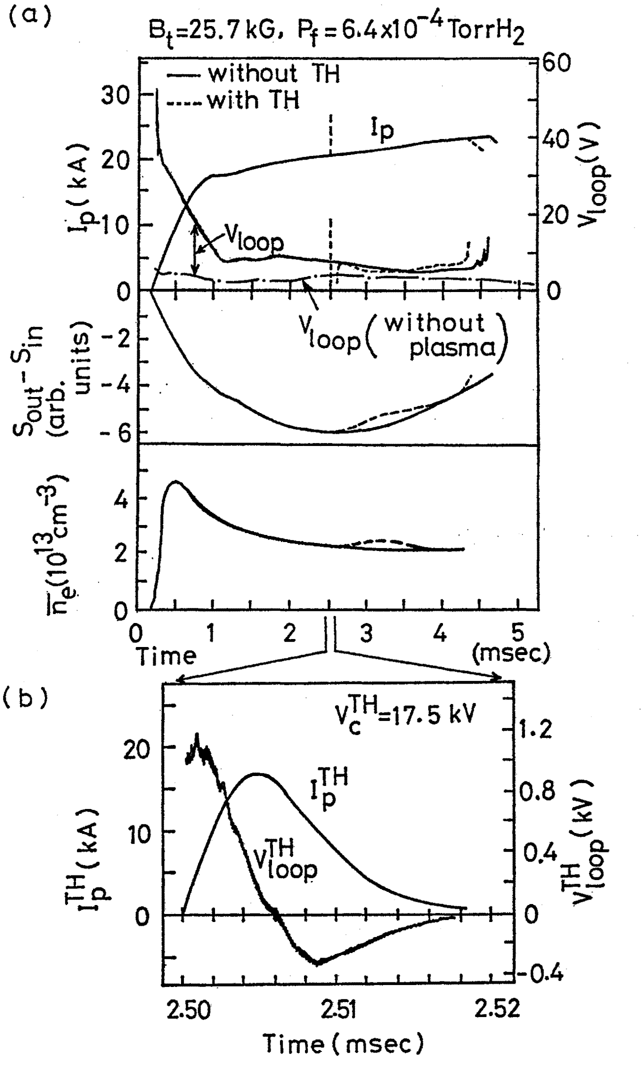

Fig. 1 (a): Discharge characteristics of both cases without (solid curves) and with the positive heating pulse (broken curves), where B_t=25.7 kG, filling pressure P_f=6.4× 10^{-4} Torr for hydrogen and charging voltage for turbulent heating V_c^{TH}=17.5 kV. The ohmic heating current (I_p), loop voltage (V_{loop}), difference of signals of magnetic probe-pair located on the equatorial plane of torus ($S_{out}-S_{in}$), line-average electron density ($\bar{n}_e$) are shown. The heating pulse is applied at 2.5 msec of the tokamak discharge.

(b): Waveforms of the pulsed current (I_p^{TH}) and loop voltage (V_{loop}^{TH}) for turbulent heating.

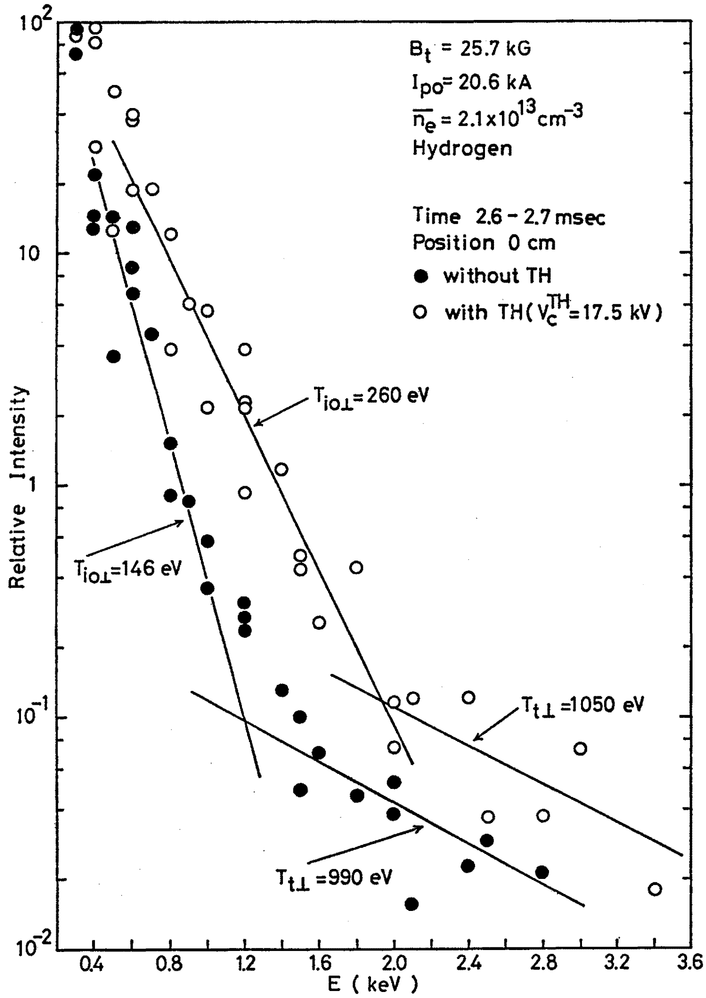

Fig. 2 Energy spectra of fast neutral atoms measured by the neutral atom energy analyzer in the equatorial plane ($z=0$) for both cases without (solid circles) and with the heating pulse (open circles). These are obtained during 0.1 msec from 2.6 to 2.7 msec. The analyzer is arranged in the perpendicular direction to the toroidal magnetic field. $T_{i0\perp}$ and $T_{t\perp}$ denote the bulk ion temperature and tail "temperature", respectively.

perature is estimated from the slope of the energy spectrum in the lower energy range ($0.4 \lesssim E \lesssim 1.2$ keV for the case without the heating pulse, and $0.4 \lesssim E \lesssim 2$ keV for that with pulse). In the case without the heating pulse, the bulk ion temperature ($T_{i0\perp}=146$ eV) follows the

Artsimovich scaling. By the heating pulse, the bulk ion temperature has attained 260 eV. The fraction of the higher "temperature" part is in order of 10^{-3} for the bulk temperature part. The high energy tail of the ion energy distribution that exists even without the heating pulse may come from the weak current driven modes such as ion cyclotron mode[16] and the various modes in the slide-away regime[17], since the streaming parameter $\langle u_d\rangle/\langle v_{\rm the}\rangle$ is considerably large as 0.20–0.25.

The time variation of bulk ion temperature at $z=0$ ($T_{i0\perp}$) is shown in Fig. 3 together with those of central electron temperature (T_{e0}) and line-average electron density ($\bar{n}_e$). The solid curves marked by "A" and broken ones marked by "B" denote the cases without and with the heating pulse, respectively. The ion temperature raised by the heating pulse decreases to the ion temperature obtained by ohmic heating alone with an e-fold decay time (τ_{*i}) of about 330 μsec. Since the characteristic decay time is expressed by the relation $\tau_{*i}=\tau_{eq}\tau_{Ei}/(\tau_{eq}+\tau_{Ei})$, the ion energy confinement time τ_{Ei} is estimated from the relation as about

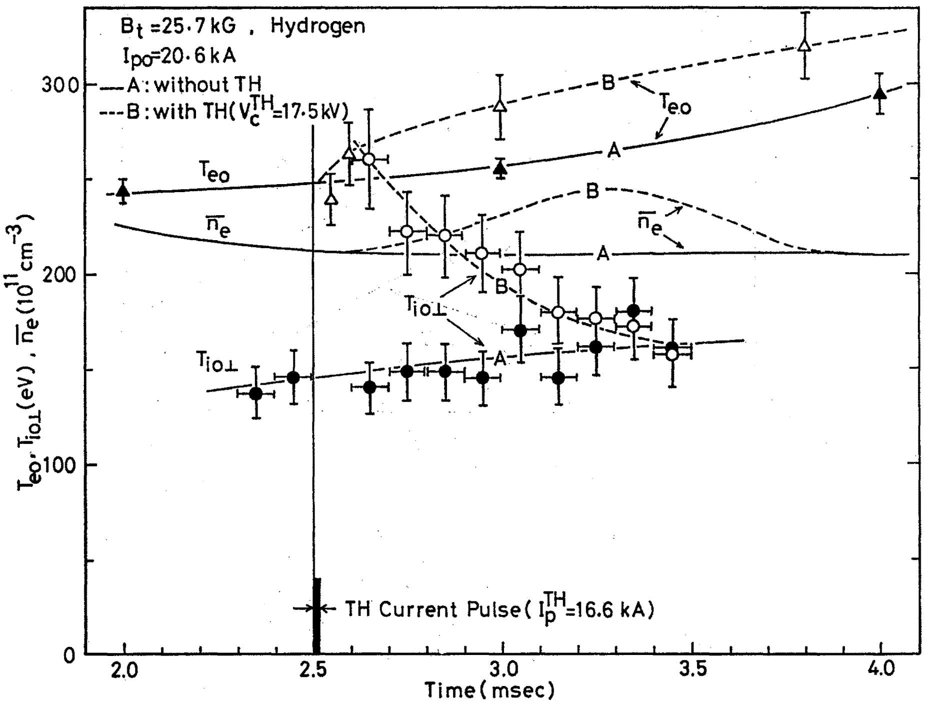

Fig. 3 Time variation of bulk ion temperature at $z=0$ ($T_{i0\perp}$), central electron temperature (T_{e0}) and electron density ($\bar{n}_e$) for both cases without (solid curves: A) and with the heating pulse (broken curves: B).

500 μsec, which agrees well with the ion energy confinement time predicted from the neoclassical transport theory[18], where τ_{eq} is the equipartition time and is about 970 μsec.

We have scanned NEA in the vertical direction from $z=+4$ cm (top) to -4 cm (bottom). Figure 4 shows the profile of ion temperature in the vertical direction $T_{i\perp}(z)$, where the solid and open circles denote the ion temperatures without and with the heating pulse, respectively. It should be noted that $T_{i\perp}(z)$ may considerably be modified from the true radial profile due to the trapped ion effect, impermeability of plasma to neutral atoms, reflection of neutral atoms by the wall and so on. From is seen from Fig. 4, $T_{i\perp}(z)$ in the upper region ($z>0$) is remarkably distorted by the trapped ion effect. In the lower region, the trapped

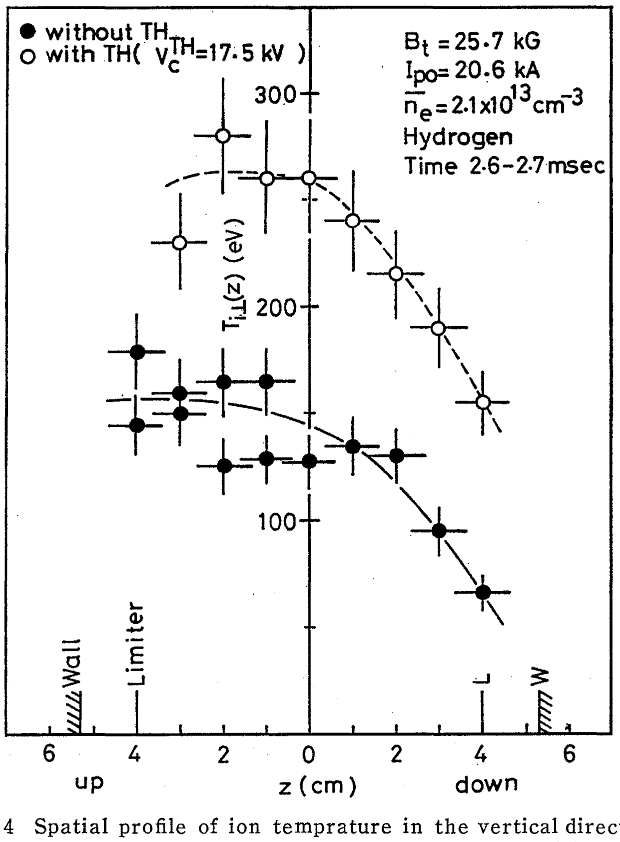

Fig. 4 Spatial profile of ion temprature in the vertical direction. The solid and open circles denote the cases without and with the heating pulse, respectively. These profiles are obtained during 0.1 msec from 2.6 to 2.7 msec. The effect of trapped ions on the ion temperature profile will be neglected in the lower region ($z \leqq 0$).

ion effect can be neglected. However, $T_{i\perp}(z)$ in the lower region may still be modified by the impermeability effect and wall-reflection. The former affects the ion temperature profile in the central region with the higher electron density, and the latter affects that near the plasma surface. In this experimental condition ($\bar{n}_e \simeq 2.1\times 10^{13}\mathrm{cm}^{-3}$), the characteristic parameter $\bar{n}_e \sigma_{cx} a$ which is the measure of the impermeability of plasma to neutral atoms is sufficiently smaller than unity in the relevant energy range ($E=0.4$–$2\,\mathrm{keV}$)[19], where σ_{cx} and a are the cross-section for resonant charge exchange of hydrogen ions and atoms, and minor plasma radius, respectively. Therefore, the correction by the impermeability effect is considered to be within 10% even in the plasma center. On the other hand, the considerably high ion temperature near the plasma surface in Fig. 4 suggests the wall-reflection effect. Though $T_{i\perp}(z)$ in the lower region is modified by the above-mentioned wall-reflection effect, it is considered from the comparison between the profiles in both cases without and with the heating pulse that the bulk ions are heated up over the whole plasma region.

In Fig. 5, the relation between the central ion temperature ($T_{i0\perp}$) during 0.1 to 0.2 msec after the heating pulse and the charging voltage of the capacitor for turbulent heating (V_c^{TH}) is investigated. The ion temperatures for both polarities (positive and negative) increase in proportion to $[V_c^{TH}]^{\alpha}(\alpha=1$–$2)$ up to the certain value of V_c^{TH}. The increase in ion temperature, however, is limited by current disruption due to reduction to $q(a)\simeq 2$ in the case of the positive polarity and by lack of MHD equilibrium due to vanishing of a total plasma current in the negative one, respectively. In the case of positive polarity, the ratio of the calculated Spitzer conductivity with the trapped-electron correction for hydrogen plasma to the experimentally obtained conductivity $\langle\sigma_{SP1}\rangle/\langle\sigma_{\exp}\rangle=0.5$–$1.5$ and this fact seems to suggest the feature in the slide-away regime. On the other hand, the above ratio in the negative polarity case increases up to 1.5–3, and that can be explained by the impurity influx. Moreover, the soft X-ray measurement by PIN diode also suggests the considerable amount of impurity influx by the negative pulse.

The increment of ion temperature $\triangle T_{i0\perp}$ is derived from Fig. 5 as a function of ratio $I_p^{TH}/\bar{n}_e$, where I_p^{TH} and $\bar{n}_e$ are the plasma current induced by the heating pulse and line-average electron density, respectively (Fig. 6). In the positive polarity case, $\triangle T_{i0\perp}$ increases linearly with $I_p^{TH}/\bar{n}_e$, if I_p^{TH} is not limited by the current disruption in tokamak plasma. The dependence of $\triangle T_{i0\perp}$ on $I_p^{TH}/\bar{n}_e$ in the negative polarity case is considerably different from that in the positive one, that is, $\triangle T_{i0\perp}$ increases with a quadratic dependence of $I_p^{TH}/\bar{n}_e$ and reaches the maximum. When $|I_p^{TH}/\bar{n}_e|$ is increased still more, $\triangle T_{i0\perp}$ decreases rapidly due to the remarkable

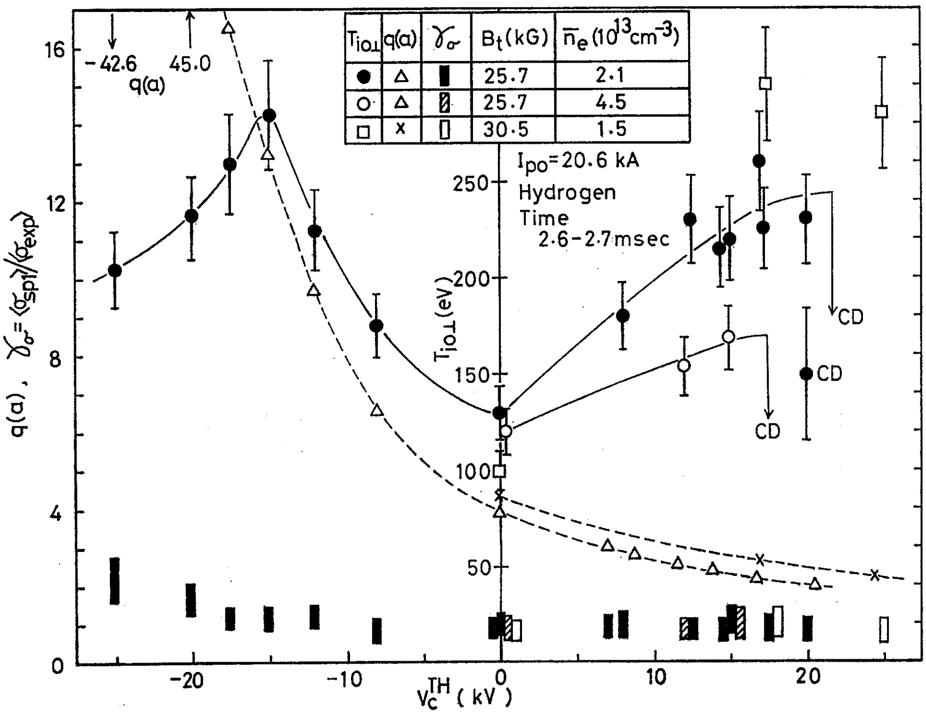

Fig. 5 Relation between $T_{i0\perp}$ and V_c^{TH}, where V_c^{TH} is the charging voltage of the capacitor for turbulent heating. This relation is derived from the data obtained from 2.6 msec to 2.7 msec. The parameters q (a) and γ_σ are the safety factor for the total plasma current $(I_p+I_p^{TH})$ and the ratio of the calculated Spitzer conductivity for hydrogen plasma with the trapped electron correction $\langle\sigma_{SP1}\rangle$ to the experimentally obtained one $\langle\sigma_{\exp}\rangle$, respectively, where $T_e(r)=T_{e0}(1-(r/a)^2)^n(n=1-2)$ and $n_e(r)=n_{e0}(1-(r/a)^2)$. The sign "CD" means the discharge terminated by the current disruption within about 20 μsec from the heating pulse.

reduction of rotational transform of magnetic field lines.

4. Discussion

The efficient ion heating observed in TRIAM-1 will be explained by the excitation of the various current-driven modes. The relevant current-driven modes in turbulent heating of tokamak plasma are the ion acoustic mode[16], ion cyclotron mode[16], lower hybrid mode in the slide-away regime[17] and so on. The excitation of these modes sensitively depends on the streaming parameter $\langle u_d\rangle/\langle v_{the}\rangle$ and/or the temperature ratio T_e/T_i. In the discharge shown in Fig. 1, the streaming parameter

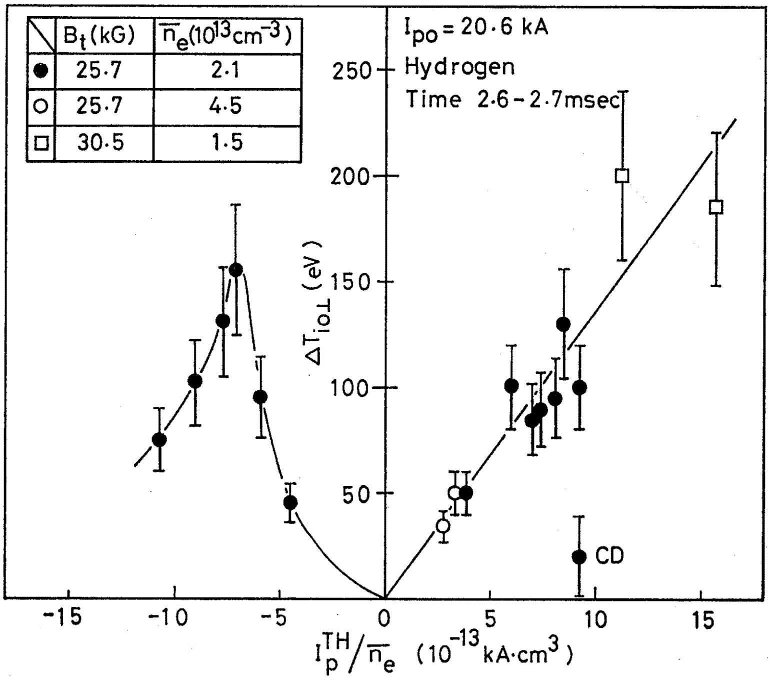

Fig. 6 Dependence of the increment of central ion temperature ($\triangle T_{i0\perp}$) on $I_p^{TH}/\bar{n}_e$ derived from Fig. 5.

is about 0.25 at the time just before the heating pulse, and amouns to 0.5 at the peak of the pulsed current, assuming that the pulsed current penetrates completely into the plasma and no heating of electrons occurs where $T_e(r)=T_{e0}(1-(r/a)^2)^2$ and $n_e(r)=n_{e0}(1-(r/a)^2)$. On the other hand, the temperature ratio at the center T_{e0}/T_{i0} is not so large as $T_{e0}/T_{i0}\simeq 1.8$ just before the heating pulse. Therefore, the ion cyclotron mode rather than the ion acoustic mode may easily be excited in this experimental condition[16]. The excitation of the ion cyclotron mode can explain the observed efficient ion heating. There is also a possibility to be able to explain the above-mentioned ion heating by the slide-away effect studied in Alcator[20] and TM-3[21].

In this experiment, the elctron temperature is monitored on only plasma axis at the time except for the applied interval of the heating pulse, so that we cannot clearly evaluate how much the electrons are heated up in the whole plasma region. From the time behaviour of T_{e0} in Fig. 3, however, the information as to electron heating can be derived to a certain extent. If the radiation loss is not dominant in comparison with the electron thermal conduction in the outer region where another peak of electron temperature will be produced by the heating pulse, the central electron temperature T_{e0} will increase with the characteristic time related to the electron thermal conduction time. The increasing time of $T_{e0}(\tau_{*e})$ is roughly estimated by the following equation $\tau_{*e} \simeq \tau_{eh}^{in}/(1-\alpha_h)$, where τ_{eh}^{in} and α_h are the inward electron thermal conduction time and the ratio of the electron power loss to the wall to the electron power transported inwardly, respectively. The inward electron thermal conduction time τ_{eh}^{in} is about 100–200 μsec, which is estimated from the neoclassical electron thermal conduction enhanced by 2000 times. The increasing time $\tau_{*e} \simeq 350\,\mu$sec derived from Fig. 3 can be realized on $\tau_{eh}^{in}=100$–$200\,\mu$sec with $\alpha_h=0.4$–0.7. The decrease in V_{loop} shown in Fig. 1 is consistent with the abovementioned increase of T_{e0}. Moreover, the increase of $\bar{n}_e$ shown in Fig. 1 is considered to be due to the impurity influx which comes from the energy loss to wall $(\alpha_h>0)$ of the input electron energy by the heating pulse.

5. Conclusion

In TRIAM-1, when the relatively low electric field ($E_D \ll E_t \lesssim 10$ V/cm) is applied in the course of the typical tokamak plasma, ions are efficiently heated up by about two times over the whole plasma region without deterioration of the confinement properties of tokamak plasma. The raised ion temperature decreases with a characteristic decay time related to the ion energy confinement time predicted from the neoclassical transport theory. The above phenomena are observed in both polarities of the current pulse with respect to the ohmic heating current, and the simple relation between the increment of ion temperature $\triangle T_{i0\perp}$ and the ratio $I_p^{TH}/\bar{n}_e$ is derived. This relation shows that $\triangle T_{i0\perp}$ increases linearly or quadratically with respect to $I_p^{TH}/\bar{n}_e$ within the certain critical value of I_p^{TH}. The ion acoustic mode, ion cyclotron mode, and lower hybrid mode in the slide-away regime are considered as the current-driven modes which will be related to the observed efficient ion heating. It is concluded from the above results that the turbulent heating is effective for heating tokamak plasmas. Moreover, it is expected that the more efficient ion heating is achieved by the sequential multi-heating pulses[9] with the time interval which is sufficiently shorter than the ion energy confinement time.

Acknowledgements

The authors would like to express their gratitude to Professor N. Yajima and Professor K. Kitajima for their continuous encouragements and also to Mr. S. Kawasaki and Mr. H. Nakashima for the technical assistance of the experiment.

References

1) L. A. Berry, C. E. Bush, J. L. Dunlap, P. H. Edmonds, T. C. Jernigan, J. F. Lyon, M. Murakami, W. R. Wing, in Plasma Phys. and Controlled Nucl. Fusion Research (Proc. 5th Intern. Conf. Tokyo, 1974) **1**, IAEA Vienna (1975) 101.
2) Equipe TFR, Nucl. Fusion **18** (1978) 1271.
3) H. Eubank, R. Goldston, V. Arunasalam, M. Bitter, K. Bol, D. Boyd, N. Bretz, J. P. Bussac, S. Cohen, P. Colestock, S. Davis, D. Dimock, H. Dylla, P. Efthimion, L. Grisham, R. Hawryluk, K. Hill, E. Hinnov, J. Hosea, H. Hsuan, D. Johnson, G. Martin, S. Medley, E. Meservey, N. Sauthoff, G. Schilling, J. Schivell, G. Schmidt, F. Stauffer, L. Stewart, W. Stodiek, R. Stooksberry, J. Suckewer, G. Tait, M. Ulrickson, S. von Goeler, M. Yamada, in Plasma Phys. and Controlled Nucl. Fusion Research (Proc. 7th Intern. Conf. Innsbruck, 1978) **1**, IAEA, Vienna (1979) 167.
4) P. Blanc, W. Hess, G. Ichtchenko, P. Javel, P. Lallia, C. Mahn, T. K. Nguyen, W. Ohlendorf, G. W. Pacher, H. D. Pacher, S. Takamura, G. Tonon, J. G. Wegrowe, in Plasma Phys. and Controlled Nucl. Fusion Research (Proc. 6th Intern. Conf. Berchtesgaden, 1976) **3**, IAEA, Vienna (1977) 49.
5) H. Takahashi, C. C. Daughney, R. A. Ellis, Jr., R. J. Goldton, H. Hsuan, T. Nagashima, F. J. Paoloni, A. J. Sivo, S. Suckewer, Phys. Rev. Lett. **39** (1977) 31.
6) S. M. Hamberger, J. Jancarik, L. E. Sharp, D. A. Aldcroft, A. Wetherell, in Plasma Phys. and Controlled Nucl. Fusion Research (Proc. 4th Intern. Conf. Madison, 1971) **2**, IAEA, Vienna (1972) 37.
7) A. Hirose, Y. Amagishi, M. R. Shubaly, H. M. Skarsgard, B. F. White, in Plasma Phys. and Controlled Nucl. Fusion Research (Proc. 5th Intern. Conf. Tokyo, 1974) **3**, IAEA, Vienna (1975) 299.
8) R. D. Bengtson, K. W. Gentle, J. Jancarik, S. S. Medley, P. Nielsen, P. Phillips, Phys. Fluids **18** (1975) 710.
9) H. De Kluiver, C. J. Barth, H. J. B. M. Brocken, J. J. L. Caarls, B. De Groot, H. W. Kalfsbeek, H. W. Piekaar, A. Ravestein, W. R. Rutgers, B. De Stigter, H. W. H. Van Andel, H. W. Van Der Ven, in Plasma Phys. and Controlled Nucl. Fusion Research (Proc. 7th Intern. Conf. Innsbruck, 1978) **2**, IAEA, Vienna (1979) 639.
10) N. Hiraki, S. Itoh, Y. Kawai, K. Toi, K. Nakamura, O. Mitarai, S. Kawasaki, H. Nakashima, Report of Research Institute for Applied Mechanics (Kyushu Univ.) **27** (1979), 85.
11) K. Toi, S. Itoh, Y. Kawai, N. Hiraki, K. Nakamura, O. Mitarai, in Proc. of USSR-Japan Joint Seminor on Plasma Diagnostics, Nagoya (1979), to be published.
12) U. Ascoli-Bartoli, G. Bosia, G. Boxman, P. Brossier, B. Coppi, L. De Kock, B. Meddens, B. Montgomery, A. Oomens, L. Ornstein, R. Parker, L. Pieroni, S. Segre, R. Taylor, P. Van Der Laan, R. Van Heyningen, in Plasma Phys. and Controlled Nucl. Fusion Research (Proc. 5th Intern. Conf. Tokyo, 1974) **1**, IAEA, Vienna (1975) 191.
13) K. Nakamura, N. Hiraki, K. Toi, S. Itoh, Report of Research Institute for Applied Mechanics (Kyushu Univ.) **27** (1980), to be published.
14) O. Mitarai, H. Nakashima, K. Nakamura, N. Hiraki, K. Toi, Y. Kawai, S. Itoh, Report of Research Institute for Applied Mechanics (Kyushu Univ.) **27** (1980), to be published.
15) O. Mitarai, Report of Research Institute for Applied Mechanics (Kyushu

Univ.) **27** (1979), 71.
16) J. M. Kindel, C. F. Kennel, J. of Geophys. Res. **76** (1971) 3055.
17) B. Coppi, F. Pegoraro, R. Pozzoli, G. Rewoldt, Nucl. Fusion **16** (1976) 309.
18) P. E. Stott, Plasma Phys. **18** (1976) 251.
19) Yu. N. Dnestrovskij, S. E. Lysenko, A. I. Kislyakov, Nucl. Fusion **19** (1979) 293.
20) A. A. M. Oomens, L. Th. M. Ornstein, R. R. Parker, F. C. Schüller, R. J. Taylor, Phys. Rev. Lett. **36** (1976) 255.
21) V. V. Alikaev, K. A. Razumova, Yu. A. Sokolov, Sov. J. Plasma Phys. **1** (1975) 303.

(Received December 3, 1979)